INTRAGASTRIC STRUCTURING OF ANIONIC POLYSACCHARIDE KAPPA-CARRAGEENAN FILLED GELS UNDER PHYSIOLOGICAL *IN VITRO* DIGESTION CONDITIONS

Soukoulis Christos*[,1], Ian D. Fisk[2], Heng-Hui Gan[3] and Lucien Hoffmann[1]

[1]Environmental Research and Innovation Department (ERIN), Luxembourg Institute of Science and Technology (LIST), 5, avenue des Hauts-Fourneaux, L-4362, Esch-sur-Alzette, LUXEMBOURG

[2]Division of Food Sciences, School of Biosciences, University of Nottingham, LE12 5RD, Sutton Bonington, UNITED KINGDOM

[3]Division of Food Science and Nutrition, School of Chemical and Life Sciences, Nanyang Polytechnic, 180 Ang Mo Kio Avenue 8, 569830, SINGAPORE

*Author to whom correspondence should be sent

Dr. Eng. Christos Soukoulis

E-mail address: christos.soukoulis@list.lu

Tel: +3522758885033

ABSTRACT

In the present work, sodium alginate (SA), low methoxyl pectin (PEC) and κ-carrageenan (κ-CAR) were evaluated for their intragastric structuring ability by means of light and dynamic oscillatory rheology. SA and PEC solutions, their Ca^{2+} complexed gel analogues as well as their binary blends with ionically or thermally set sheared κ-CAR gels, were subjected to *in vitro* orogastric conditions. SA and PEC – Ca^{2+} complexed sheared gels exerted the highest vulnerability to digestive fluid exposure due to the dialysis of egg-box dimer structures via proton-calcium exchange. Incorporation of SA and PEC systems to κ-CAR gels prevented the loss of mechanical strength of the gastric gels due to the ability of κ-CAR to undergo spontaneous gelation in the presence of Na^{+} and K^{+} ions. Binary blends of SA and PEC – Ca^{2+} complexed sheared gels with κ-CAR-Ca^{2+} gels exerted a significantly lower mechanical strength loss sensitivity against pH and counterion composition of the gastric fluids.

Keywords: alginates; pectins; intragastric structuring; pre-absorptive digestion conditions; acid gelation; ionotropic gelation.

1. INTRODUCTION

Over the last decades the prevalence of obesogenic lifestyle associated with the consumption of highly calorific food products, limited uptake of essential micronutrients and dietary fibre, as well as restricted physical activity have led to an alarming increase of obesity and obesity related health complications (Lake and Townshend, 2006). As result, health disease such as type II diabetes, metabolic syndrome, hypertension, coronary artery disease, stroke, osteoarthritis, liver and gall bladder disease, and obstructive sleep apnoea have been evidenced (Kopelman, 2007). In addition, the association of obesity to several forms of cancer such as endometrial, kidney, postmenopausal breast and colocteral adenoma has been reported (Kopelman, 2007; Vigneri et al., 2006). Modulation of eating behaviour via suppressing appetite and controlling the dietary and calorific value of food are widely recognised as effective strategies to counteract obesity. As for appetite suppression, it has been demonstrated that satiety is a responsive construct of the combination of environmental, physiological and neurobiological signalling which involves food choice and intake based on the cross-modal orosensory perception response, as well as pre-absorptive gastric stretching and emptying, suppression of digestive enzymes activity) and post absorptive (macro- and micro-nutrients absorption, regulation of the gut microbiota) parameters (Bellisle, 2008; Chambers et al., 2015; Fiszman and Varela, 2013a, 2013b; Llewellyn and Wardle, 2013).

Food macromolecules including proteins, dietary fibre and lipids are known as having a pivotal impact on satiety signalling; however, this is generally attained via different mechanistic physiological and neurobiological pathways (Fiszman and Varela, 2013b). As concerns to dietary fibre, their satiety suppression effectiveness stems from their chemical and functional aspects such as thickening and gelling ability, water and oil holding capacity, fermentability/digestibility, absorption and mucoadhesivity (Brownlee, 2011; Fiszman and Varela, 2013a, 2013b; Kristensen and Jensen, 2011). In a pre-absorptive digestion context,

dietary fibre can induce a plausible suppression of appetite via their ability to prolong orosensory exposure (oral processing/mastication, secretion of saliva and gastric juice) and to modulate the gastric response to food ingestion, e.g. activation of stomach mechanoreceptors triggering stomach distension due to intragastric structuring, reduction of gastric enzymes activity and delay of gastric emptying. Therefore, soluble dietary fibre exerting a fair thickening ability and/or self- or co-structuring (in the presence of other macronutrients) ability under acidic conditions, such as pectins, seaweed extracts (alginates and carrageenans), root extracts (konjac gum), microbial synthesised gums (curdlan and gellan) and cellulose derivatives (HPMC, CMC), have been scrutinised as potential intragastric structuring materials (Borreani et al., 2016; Bradbeer et al., 2014; Fiszman and Varela, 2013a; Garrec et al., 2013; Logan et al., 2015; Morell et al., 2014; Soukoulis et al., 2016; Spyropoulos et al., 2011; Zhang et al., 2014). In addition, biopolymer assisted structural and interfacial engineering methods have also been developed to reduce the energy density and promote satiety response of staple processed food (Norton et al., 2006 & 2015). For example, crosslinked gel networks (hydrogels) and ionotropically gelled microparticulates (fluid gels), protein-polysaccharide assembled structures, as well as highly viscosified aqueous systems (w/w) or o/w emulsions are only some of the structurally bespoke food models promoting satiation response via their intragastric structuring ability (Norton et al., 2015). When it comes to scrutinising the intragastric ability of biopolymer structure engineered food models, adopting physiological pre-absorptive digestion conditions is of paramount importance. Soukoulis and co-workers (2016) have demonstrated that the adoption of a harmonised *in vitro* digestion protocol (INFOGEST) was associated with evidently diversified structuring performance of sodium alginate based o/w emulsions throughout gastrointestinal passage. Therefore, parameters such as the pH fluctuation due to human host physiological diversity and stomach fullness state, as well as the counterions complexity of the individual simulating pre-absorptive digestive fluids

(including the oral phase) should be considered as validating criteria of the foreseen intragastric structuring performance of food biopolymers.

In the present work we aimed to investigate the intragastric structuring ability of gel composites comprising anionic polysaccharides as the responsive construct of intrinsic (ionotropic, random to ordered coil and acid self-induced gelling ability) and extrinsic (pH of the gastric chymes, concentration and ionic strength of the simulating pre-absorptive digestive fluids) parameters. The morphological and mechanical characteristics of the gastric chymes were assessed by means of optical microscopy and dynamic oscillatory rheology respectively.

2. MATERIALS AND METHODS

2.1 *Materials*

Low viscosity sodium alginate (250 mPa·s, 2% w/w in water at 25°C, M/G ratio = 1.6, mannuronic to guluronic acid content 61-31, $M_w = 1.43 \times 10^5$ g mol^{-1}), κ-carrageenan (5-25 mPa·s, 0.3% w/w in water at 25°C), anhydrous calcium carbonate, δ-glucono-lactone, and porcine pepsin (ca. 474 U/mg) were purchased from Sigma Aldrich (Leuven, Belgium). All other chemicals, unless otherwise stated, were from the same supplier and of analytical grade quality. Low calcium reactivity apple pectin (45 % degree of esterification, 80% galacturonic acid content, $M_w = 2 \times 10^5$ g mol^{-1}) was kindly provided as a gift from Herbstreith and Fox GmbH (Neunbürg, Germany). All biopolymers listed were used without any further purification.

2.2 *Preparation of the biopolymer based solutions and Ca^{2+} mediated gel systems*

Two grams of biopolymer (sodium alginate, κ-carrageenan, or pectin) were dispersed into 200 mL of deionised 18 MΩ water (Millipore, USA), heated at 80 °C, kept at the same temperature for 1 h to allow complete dissolution and then the obtained aliquots were cooled at 50 °C and left to fully hydrate overnight under constant magnetic stirring. To prevent microbial spoilage,

a small amount of sodium azide (0.002% w/w) was added. One hundred mL aliquots of sodium alginate, pectin and κ-carrageenan solutions (2% w/w) were mixed with anhydrous calcium carbonate in order to achieve a final concentration of 40 mM. The biopolymer solutions were successively ultrasonicated (5 min, 90% amplitude, UP200S, Hielscher GmbH, Teltow, Germany) to ensure uniform distribution of $CaCO_3$. Finally, the biopolymer solutions were mixed with δ-glucono-lactone (at a 2:1 GDL to $CaCO_3$ ratio), covered with aluminium foil and kept under magnetic agitation (1000 rpm) at 50 ˚C for 6 h to allow ionotropic gelation of the biopolymers triggered via the *in situ* release of Ca^{2+} ions for 6 h. Evaporated water was added back and the gels were cooled at ambient temperature under stirring (20±2 ˚C). A similar approach was also used in the case of thermally set κ-carrageenan systems, i.e. the heated solutions were left to cool down (ca. 2 ˚C/min) to ambient temperature under constant magnetic agitation as previously described. Binary blends (1:1) of the Ca^{2+} complexed sodium alginate and pectin with either ionically or thermally set κ-carrageenan were also prepared. All biopolymer comprising systems were stored overnight at ambient temperature before carrying out the *in vitro* pre-absorptive digestion experiments.

2.3 *In vitro pre-absorptive digestion of the biopolymer solutions and Ca^{2+} mediated gels*

The gastric structuring ability under simulated physiological conditions was studied adopting the INFOGEST static standardised *in vitro* model as previously described by Minekus et al. (2014). In brief, 5 g of the biopolymer system (solution or gel), preconditioned at 37±1 ˚C, were transferred into 50 mL plastic centrifuge tubes and mixed with 5 mL of simulated salivary fluid (SSF) (pH = 7, K^+ = 18.8, Na^+ = 13.6, Mg^{2+} = 0.15, Ca^{2+} = 1.5 mM). The obtained oral phase was successively mixed with 10 mL simulated gastric fluid (SGF) (pH = 2, K^+ = 7.8, Na^+ = 72.2, Mg^{2+} = 0.1, Ca^{2+} = 0.15 mM) and incubated at 37 °C for 1 h into a shaking water bath (GFL GmbH, Germany) operated at 100 rpm simulating a physiologically achievable antral shear rate (Vardakou et al., 2011). Simulated gastric chyme systems were cooled down

151 to 25 °C and were successively characterised by means of dynamic oscillatory rheology. *In*
152 *vitro* digestion experiments were carried out in triplicate.
153 In addition, a duplicate batch of model gastric chymes adjusted to a pH ranging from 1 to 4,
154 corresponding to stomach conditions varying from the fasted (starvation) to fed (full stomach)
155 state respectively, was also prepared adopting either physiological (systems diluted with SSF
156 & SGF) or non-physiological (systems diluted exclusively with Millipore water) pre-absorptive
157 digestion conditions.

158 **2.4 *Dynamic oscillatory rheological measurements***

159 Dynamic oscillatory rheological measurements of the initial biopolymer aqueous systems as
160 well as of the obtained gastric chymes were carried out in an Anton-Paar rheometer (MCR 302,
161 WESP, Graz, Austria). Initial biopolymer aliquots were measured using a cone plate geometry
162 (CP50-1) whilst the gastric chyme suspensions were analysed by means of double gap
163 concentric cylinder geometry (DG 26.7). All measurements were performed at 25 ± 0.03 °C.
164 Strain-sweep (0.001 to 1000%) measurements of the biopolymer aliquots and gastric chymes
165 were carried out at 1Hz to determine the linear viscoelastic region (LVR). Therefore, the
166 viscoelastic properties of all biopolymer systems were determined by small frequency
167 amplitude sweeps (0.1 to 10 Hz) at a constant strain of 0.1%.
168 Thermo-oscillatory scans at a constant strain of 0.1% and frequency of 1 Hz were also carried
169 out to investigate the melting behaviour of the biopolymers. To prevent water evaporation the
170 cone-plate edge was covered with a small amount of silicon oil. A cooling-heating protocol
171 was applied as follows: a) heating from 10 to 70 at 2˚C/min, b) holding at 70˚C for 5 min and
172 c) cooling from 70 to 10˚C at 2˚C/min. The elastic modulus (G´) and storage modulus (G´´)
173 curves crossover points, at heating and cooling step were calculated to define melting and
174 gelation temperature (midpoint) of the biopolymer systems, respectively (Suppl. Table 1).

175 **2.5 *Light microscopy***

The structure conformational changes of the biopolymer fibres during the pre-absorptive digestion conditions (saliva and gastric phases) were qualitatively assessed by means of optical microscopy. A small amount (ca. 1 mL) of the individual biopolymer containing gastric chyme was mixed with either 0.25 mL of toluidine blue solution (0.05% w/w in distilled water) or 0.25 mL of saffronin solution and vortexed for 30 s. Toluidine blue was used to stain κ-carrageenan whereas saffronin was used to stain sodium alginate and pectin containing systems. A 1:1 toluidine blue to saffronin mixture was used to stain the binary biopolymer based gastric chymes. Then, ca. 200 μL of the stained biopolymer aliquot was deposited on a glass slide and covered carefully by a glass cover slip so to avoid the entrapment of air bubbles. Samples were visualised at a magnification of 10× using a Zeiss optical microscope (Axio Vert A1, Zeiss GmbH, Germany).

2.6 *Statistical analyses*

Normal distribution of data and equality of variance were verified by normal distribution plots and box-plots, respectively. One way ANOVA was performed on complex viscosity data of the simulated gastric chymes in order to evaluate the significance of pH and ionic strength conditions. All analyses were carried out using SPSS v.19 statistical software (IBM Inc., Chicago, IL, USA).

3. RESULTS AND DISCUSSION

3.1 Thermo-oscillatory characterisation of the biopolymer aliquots

The biopolymer aqueous systems were subjected to thermo-oscillatory scanning within the linear viscoelasticity region (frequency 1Hz, strain 0.1%) to assess their mechanical response on their mixing with simulated pre-absorptive digestion fluids (saliva and gastric juice) as well as to determine the physical state transitions, i.e. sol to gel, during the fabrication of the sheared biopolymer gels (Fig. 1). Corroborating the literature data, only κ-carrageenan (CAR) systems exerted a clear sol-gel transition occurring at ca. 39˚C as result of its ability to undergo random

coil to double helix structure conformation (Tecante and Nez Santiago, 2012). As for sodium alginate (SA) and apple pectin (PEC), systems did not exert any distinct physical state transition retaining their domineering viscous-like character across the 10-70˚C temperature range (Suppl. Table 1, Fig. 1). Nevertheless, in the case of PEC, rheological spectra exhibited significant hysteresis which possibly is associated with the conformational reorganisation of pectin aggregates as function of temperature. Indeed, Muhidinov et al. (2011) demonstrated that by heating PEC aqueous systems from 20 to 60˚C, Higgins coefficient (K_h) was reduced attaining a minimum value around 40˚C which was primarily attributed to the disintegration of pectin aggregates. Further increase of temperature resulted in the increase of K_h indicating the restructuring of protein molecules into small compact structures.

Ionotropic (Ca^{2+}) gelation of the biopolymer did not modify significantly the profile of the thermo-rheological spectra in the case of SA and CAR. In the latter case, a more pronounced hysteresis between the melting and cooling curves was observed probably due to the occurring gel-sol-gel transitions, i.e. de-assembly of the aggregated double helices to form random biopolymer coils and vice versa (Kara et al., 2003). In addition, upon heating, CAR-Ca^{2+} sheared gels retained their domineering solid like behaviour (G´>G´´) in the entire temperature range suggesting a partial de-assembly of the double helices contrarily to pure CAR systems. On the other hand, ionic gelation of PEC resulted in a significant decrease of their responsiveness to temperature e.g. hysteresis loop area.

Blending the ionic sheared gels (SA, PEC) with the sheared κ-carrageenan gels (thermoset and ionotropically set) at the ratio of 1:1 (Fig. 1c,d), resulted to hybrid biopolymer gel structures characterised by a domineering solid like behaviour (G´>G´´) and larger hysteresis loop areas. Although the absence of sol-gel transitions is sufficiently rational for sheared ionic gel mixtures, in the case of SA-Ca^{2+}/CAR and PEC-Ca^{2+}/CAR gels, the dimer structures exerted a governing influence over the structuring ability of κ-carrageenan. On the contrary, in SA/CAR

and PEC/CAR gels, sol-gel transitions took place (in the range of ca. 20 to 36˚C), indicating the unobstructed ability of κ-carrageenan to undergo coil to double helix structure conformational changes. Therefore, blending of the former gels with the oral and gastric fluids would expectedly induce a remarkable suppression of the melting points. Indeed, thermo-oscillatory rheological characterisation of κ-carrageenan gels adopting a 4-fold dilution protocol (simulating mixing with oral and gastric fluids) with deionised water revealed a considerable suppression of the melting and gelation temperature points, i.e. ca. 28 and 31 ˚C, respectively (data not shown).

3.2 Viscoelastic profiling of the biopolymer aqueous systems

The major physical state aspects of the biopolymer gels were assessed by means of dynamic oscillatory rheology (frequency sweeps) in the LVR (Fig. 2) at ambient (25 °C) temperature. As concerns the individual biopolymer aqueous systems (Fig. 2a), only κ-carrageenan exhibited a domineering solid-like behaviour (G´>G´´). A predominant liquid-like behaviour was observed for SA (G´<<G´´) indicating the sterically hindered interaction of the biopolymer chain segments (Ma et al., 2014), whilst a rather viscous liquid-like behaviour (G´<G´´, loss factor (tanδ)<1.5) was observed in the case of PEC, with both moduli being fairly frequency dependent; the latter is representative of topological interaction (hydrogen bonding and hydrophobic interactions) of pectin side chain segments (Ström et al., 2014). When biopolymers underwent Ca^{2+} complexation (Fig. 2b), an evident increase of the storage moduli was achieved, which can be attributed to the aggregation of the intermolecular junctions of the either egg-box (SA, PEC) or double helix (CAR) dimer structures (Draget et al., 2006; Fraeye et al., 2009; MacArtain et al., 2003). As concerns the biopolymer type, SA-Ca^{2+} sheared gels experienced an almost 6-order increase of G´, far higher than PEC-Ca^{2+} (> 2.5-order), and CAR-Ca^{2+} (<1.5 order). This appears to be rational considering the low Ca^{2+} reactivity of PEC due to its rather high degree and random pattern of methoxylation (Fraeye et al., 2009). For

CAR, the presence of Ca^{2+} promotes the aggregation of the junction zone (which are also formed in the case of the sheared thermoset gels) resulting to the formation of a fine network without superstrands and therefore the observed differences in the G´ values were rather moderate (Hermansson et al., 1991).

As for the binary biopolymer gel systems comprising thermoset κ-carrageenan sheared gels (CAR), a cooperative effect in terms of viscoelasticity was observed. All systems exerted a dominant solid like character (G´>G´´) of low sensitivity to oscillation frequency indicating the formation of true gel structures (Picout and Ross-Murphy, 2003). As expected, SA based binary systems were the most responsive to κ-CAR presence. It should be also noted that in the case of SA-Ca^{2+} and PEC-Ca^{2+} based blends, the G´ values achieved were ca. 4 to 8-fold higher compared to their exclusively SA-Ca^{2+} and PEC-Ca^{2+} sheared gel analogues. It is therefore hypothesised that due to the high chemical affinity of κ-carrageenan to calcium, an electrostatic intermolecular interaction between the Ca^{2+} conveying domains of SA and PEC chain segments with the negatively charged (e.g. sulfate) side groups of κ-carrageenan might also induced. Indeed, when the binary blends composed of exclusively Ca^{2+} mediated sheared gels (Fig. 2d) were scrutinised, the storage moduli were plausibly comparable to the systems containing thermoset κ-carrageenan sheared gels.

3.3 Intragastric structuring ability of the biopolymer gels

3.3.1 Morphological aspects of gastric chymes

The gastric chymes obtained following an 1h exposure to simulated gastric fluids were assessed by means of light microscopy to assess the morphological aspects of the gel microparticulates (Figs. 3-5). In order to have a more comprehensive overview of the counterion composition impact on intragastric structuring, acidified biopolymer aliquots obtained by mixing the initial gel systems with deionised water were also microscopically analysed (Soukoulis et al., 2016). In the present work the obtained micrographs provide a tangible visualisation of the structural

traits of the particulates without offering the possibility to measure the actual volume fraction of the biopolymer microparticulates. This has also been reported previously when sheared anisotropic hydrogel microstructures compressed between the glass slide and coverslip, were visually analysed (Wolf et al., 2000).

Adopting a counterion–free digestion protocol (odd numbered micrographs) was associated with more intact biopolymer structures which consecutively results in larger hydrodynamic radii of the polymeric particulates. The prevalence of monovalent cation species (e.g. Na^+ and K^+) in the physiological simulated oral and gastric juices was associated with a remarkable modification of microstructural aspects of the gastric chymes (even numbered micrographs). As concerns the individual biopolymer (non-crosslinked) containing gastric chymes, a fair erosive effect leading to the formation of particulates of smaller hydrodynamic radius was observed (Fig. 3). This corroborates our previous findings on SA based o/w emulsions where the prevalence of monovalent cations was associated with modification of the morphological aspects of the acid self-structured biopolymer (Soukoulis et al., 2016). It has been reported that SA and PEC fibres conditioned in physiological saline undergo significant hydrodynamic volume reduction; this is due to the fibre contraction induced by salting out of the biopolymer i.e. the electrostatic repulsion between the negatively chain segments is reduced in the prevalence of the cation species (Jonassen et al., 2013; Qin, 2004). However, in all cases the biopolymer systems maintained their principal structure conformational aspects, e.g. thin layered/sheet-like, cloudy/aggregated or flocculated/fragmented for CAR, SA and PEC respectively. On the ionotropic gelation, CAR underwent the most pronounced structural changes attaining a predominantly smooth yet aggregated microstructure. Contrarily, SA-Ca^{2+} and PEC-Ca^{2+} sheared gels did not undergo any plausible microstructural changes, i.e. in both cases systems maintained their aggregated particulate form.

Use of different staining protocols allowed us to sufficiently discriminate between CAR (violet coloured) and SA or PEC (dark orange coloured) rich gel microdomains (Figs. 4&5). As for the binary biopolymer gastric chyme systems containing the thermoset sheared κ-carrageenan gels (Fig. 4), a drastic size reduction of the carrageenan rich microparticulates was achieved regardless the presence and the physical state (dissolved or ionically crosslinked) of either sodium alginate or pectin. However, no significant differences in the acid particulates' morphology were detected when the physiological gastric chymes were assessed, i.e. highly fragmented/eroded (SA/CAR and PEC/CAR) or moderately aggregated (SA-Ca^{2+}/CAR and PEC-Ca^{2+}/CAR) structures were detected. In line to the aforementioned, the exposure of the SA-Ca^{2+}/CAR-Ca^{2+} and SA-Ca^{2+}/CAR-Ca^{2+} sheared gels (Fig. 5) to highly acidic conditions, the presence of an extensively aggregated network of microparticulates was confirmed. Nevertheless, *in vitro* physiological gastric chymes exerted a finely aggregated structure compared to their counterion-free analogues which is in agreement to our previous findings. Therefore it can be postulated that the prevalence of sodium in the pre-absorptive digestion fluids has an ion-exchanging role on the both Ca^{2+} triggered dimer structures, e.g. egg-box or double helices, suppressing their intragastric structuring performance (Soukoulis et al., 2016).

3.3.2 Oscillatory rheological characterisation of the gastric chymes

For the rheological characterisation of the gastric chymes a concentric cylinder geometry was used, which has been previously reported as being relevant for the analysis of aqueous suspensions (Picout and Ross-Murphy, 2003). Although the obtained values of viscoelastic moduli of chymes cannot be directly contrasted to those of the initial gel systems (measured using cone-plate geometry), the obtained rheological spectra can still give insight to the structural changes occurring throughout the pre-absorptive digestion passage. According to the gastric chyme rheographs (Fig. 6), the acid structuring ability of the gels was highly diversified on their exposure to gastric juice conditions. As for the individual based systems, CAR exerted

the most pronounced acid structuring ability particularly in its non-crosslinked state. On the other hand, mixing of PEC systems (in solution or sheared gel form) with the simulated oral and gastric fluids resulted to a drastic reduction of the storage moduli, exhibiting a domineering viscoelastic behaviour with a crossover point of the G´, G´´ moduli at low (<1Hz) frequencies. Therefore, the latter systems should behave as predominantly low viscosity liquids under the hereby simulating antral forces (ca. 1.7 Hz). It is well established that low methoxylated pectin may undergo gelation in the presence of both divalent and monovalent cation species (Thakur et al., 1997; Yoo et al., 2003). In the latter case, parameters such as the esterification and blockiness degree, the pH and the concentration and type of cation species control the sol-gel transition (Ström et al., 2014). As refers to monovalent cations, the presence of 0.2 M of Na^+ is necessary to trigger a significant gelation (true) effect via later aggregation of pectin chains via hydrophobic and van der Waals interactions (Ström et al., 2014). In our case, the low pH of gastric chymes ($pH<pK_{a,pectin}$) together with the relatively low Na^+ (ca. 0.05 M) and the low blockiness and methoxylation degree of PEC obstruct its self-aggregation leading to a loosely structured biopolymer network which conveys the characteristics of rather weak gel only at very low frequencies that fall out the range of expected antral forces (Ström et al., 2014). On the contrary, SA dilute systems attained a clear true gel-like behaviour (G´>G´´) as result of the formation of intermolecular junctions via the hydrogen bonding of the protonated carboxyl groups of the GG blocks in a cooperative manner with polymannuronic block segments (Draget et al., 2006). When the Ca^{2+} complexed sheared gels were exposed to digestive fluids (Fig. 6b), a noticeable reduction of the mechanical strength of the gels was detected. As proposed to our previous work, the prevalence of monovalent cations triggers the ion exchange (dialysis) of Ca^{2+} by H^+ hampering the intermolecular junctions between the dimer (egg-box) or double helix structures (Draget et al., 2006, 1998; Soukoulis et al., 2016). As expected, the rheographs revealed a higher impact of the digestive fluids on the PEC-Ca^{2+} than the SA gel analogues,

350 which may be attributed to the lower chemical affinity of PEC to sodium or potassium and the
351 constrained ability of the dialysed binding sites to interact via other forms of intermolecular
352 bonding, e.g. hydrogen bonding or hydrophobic interactions (Fang et al., 2008). In the case of
353 CAR-Ca^{2+} the ca. 1.5-order reduction of the G´ modulus can be primarily attributed to digestive
354 fluids diluting effect (MacArtain et al., 2003) and at a lesser extent to the antagonistic calcium
355 exchanging activity of Na^{+} under acidic conditions reducing the aggregative bridging of the
356 double helices.
357 Gastric chymes obtained by the digestion of the binary blends of either SA/SA-Ca^{2+} or
358 PEC/PEC-Ca^{2+} with κ-CAR exhibited a persistent plateau of G´ which indicates the existence
359 of a highly entangled network comprising the anisotropic gel microparticulates (Norton et al.,
360 2006). Although storage moduli were not significantly different among samples, the loss
361 moduli were generally higher in the case of the SA based systems suggesting a higher level of
362 gel particles entanglement. In addition, the presence of CAR had a dual assisting role in terms
363 of intragastric structuring: first, it counteracted the structural losses due to the 4-fold digestion
364 fluids diluting factor, and second, it prevented the gel mechanical strength loss due to the
365 dialysis of the egg-box Ca^{2+} dimers. It is therefore postulated that the high chemical affinity of
366 CAR with K^{+} and Na^{+} present in the digestive fluids impedes fibres contraction due to H^{+}
367 induced ion exchange, facilitating chain segments interaction via hydrogen bonding (Tecante
368 and Nez Santiago, 2012). Complexation of CAR with Ca^{2+} (in the case of SA-Ca^{2+}/CAR-
369 $Ca^{2+}$and PEC-Ca^{2+}/CAR-Ca^{2+} sheared gels) was accompanied by a steep reduction of G´
370 moduli (ca. 2-order compared to the initial gel systems), yet the solid like behaviour remained
371 strongly evident. On this occasion, it is assumed that the reduction of the elasticity of the acid
372 gel microparticulates is primarily associated with the dialysis of egg-box dimer structures, and
373 secondarily with the constraining of the aggregative bridging of the CAR double helices.
374 Indeed, the gel particulates elasticity reduction in the case of the PEC-Ca^{2+} containing systems

was pronouncedly higher than the SA analogues, due to their lower calcium chemical affinity leading to a sterically favoured ion exchanging effect.

3.3.3 Impact of counterions composition and pH conditions on the complex viscosity of the gastric chymes

Evaluating the impact of counterion composition of the simulating pre-absorptive digestion fluids, gastric chymes obtained by blending the initial biopolymer systems with either physiological *in vitro* saliva and gastric fluids or deionised (MilliQ) water were rheologically characterised at 1 Hz and 0.1 % strain (Fig. 7). As clearly depicted, the prevalence of Na^+ and K^+ ions was associated with a diversified intragastric structuring performance which was biopolymer dependent. As a general trend, SA based systems were better performing in terms of acid self-structuring in the absence of counterions. In this case, the formation of intermolecular junctions between both across GG blocks and at lesser extent MM block segments is sterically favoured (Draget et al., 2006). On the contrary, the intragastric structuring ability of both individual and binary CAR based biopolymer systems was reduced on their exposure to counterion-free digestive fluids supporting our postulation that electrostatic bridging of monovalent cation species with the sulfate binding sites takes place. As for PEC, solely in the case of the ionotropically structured systems a significant reduction of the intragastric structuring performance was observed in a similar manner to SA-Ca^{2+} sheared gels. However, it should be noted, that the binary blends of the ionotropically complexed biopolymers (SA-Ca^{2+}/CAR and PEC-Ca^{2+}/CAR) were not significantly affected by the ionic composition of the digestive fluids and therefore, their intragastric performance exerts the lowest sensitivity to the implemented digestion protocol.

In a consecutive case study, we attempted to assess the magnitude of the impact of simulating pH gastric conditions, ranging from the fasted to the fed stomach state (Dressman et al., 1990), on the acid structuring performance of biopolymer aqueous systems (Fig. 8). Interestingly, the

compositional profile of the biopolymer gels was found to crucially affect the responsiveness of intragastric structuring to pH fluctuations. Specifically, the acid self-structuring performance of SA exerted a steep increase (> 3-order) in the nearly fasted stomach pH range e.g. 2-3 followed by a gradual decrease of the complex viscosity under harsh pH conditions (pH<2). This is in line with the findings of Andriamanantoanina and Rinaudo (2010) who observed an increase of the storage modulus of SA alginate solutions (in their saline form) at pH<3 reaching a maximum degree of swelling of the gel fraction at pH =2.5; then, at lower pH values a gradual decrease of the suspended gel particulates was reported. It should also be noted that at highly acidic conditions (pH<3) strong cooperative interactions with the participation of polyguluronic and polymannuronic blocks are expected to take place (Draget et al., 2006). Contrarily to SA, PEC systems exhibited an up to 2-order increase of the complex viscosity (depending on their physical state i.e. ionically complexed or free) under moderate acidic environment conditions, e.g. pH = 3. Corroborating the literature data, the acid self-structuring ability of LM PEC is maximised when pH<pK_a (ca. 2.9) and in the presence of fairly sufficient concentration of monovalent (0.2 M NaCl) cation species (Ström et al., 2014). When the responsiveness of the individual κ-CAR systems was studied, a highly diversified acid structuring performance was attained depending on their physical state; complex viscosity of CAR-Ca^{2+} gastric chymes was not significantly affected by pH changes, whilst in the case of their ionically non-complexed analogues a upper structuring plateau was reached in the 2 to 3 pH range. Reduction of the pH, resulted in a significant increase of the absolute charge of the CAR molecules facilitating the electrostatic bridging of sulfate groups with the prevalently present monovalent cation species (Tecante and Nez Santiago, 2012). When the cation binding sites of the carrageenan chains are occupied by Ca^{2+} the effect of the pH on the net charge of CAR molecules is reduced leading to lower sensitivity to pH change. On mixing κ-CAR with SA or SA-Ca^{2+} (Fig. 8b), a structuring synergy was observed, with complex viscosity of the

gastric chymes remaining at high levels in the complete fasted to moderately fed state pH region i.e. 1-3. An adverse behaviour was also attained in the case of PEC/κ-CAR systems though their structuring performance was higher in the intermediate to high pH region, e.g. 2.5-4. Finally, gel systems comprising exclusively ionotropically crosslinked biopolymers exerted a rather constrained sensitivity to pH fluctuation, a behaviour that could be primarily attributed to the modulating effect of the κ-CAR-Ca^{2+} gel component.

4. CONCLUSIONS

In summary, anionic biopolymers such as sodium alginate, κ-carrageenan and low methoxylpectin can promote *in vitro* intragastric structuring via different mechanistic pathways i.e. ionotropic gelation, acid-self structuring and thickening. As for individual biopolymer systems, SA or CAR exerted the highest structuring performance induced via cooperative junction zone formation of the homopolymeric block segments and electrostatic bridging of gastric juice monovalent ions with the sulfate binding sites respectively. Notwithstanding ionically mediated sheared gels exerted a fairly true gel character, their ability to maintain their structural aspects was diminished on their exposure to simulated digestive fluids. On the other hand, blending of SA or PEC with CAR led to a synergistic gastric structuring effect. This was primarily attributed to the ability of CAR to interact with both monovalent and divalent ions present in the gastric chymes preventing their adverse impact on acid self-structuring of SA and PEC. Finally, binary semi-solid composites comprising Ca^{2+} complexed anionic polysaccharides exhibited the most limited responsiveness to the pH and ionic composition of simulated digestive fluids.

Conflict of interest: Authors declare no conflict of interest.

5. REFERENCES

449 Andriamanantoanina, H., Rinaudo, M., 2010. Relationship between the molecular structure of
450 alginates and their gelation in acidic conditions. Polym. Int. 59, 1531–1541.
451 Bellisle, F., 2008. Functional foods and the satiety cascade. Nutr. Bull. 33, 8–14.
452 Borreani, J., Llorca, E., Larrea, V., Hernando, I., 2016. Adding neutral or anionic
453 hydrocolloids to dairy proteins under in vitro gastric digestion conditions. Food
454 Hydrocoll. 57, 169–177.
455 Bradbeer, J.F., Hancocks, R., Spyropoulos, F., Norton, I.T., 2014. Self-structuring foods
456 based on acid-sensitive low and high acyl mixed gellan systems to impact on satiety.
457 Food Hydrocoll. 35, 522–530.
458 Brownlee, I.A., 2011. The physiological roles of dietary fibre. Food Hydrocoll., Dietary Fibre
459 and Bioactive Polysaccharides 25, 238–250.
460 Chambers, L., McCrickerd, K., Yeomans, M.R., 2015. Optimising foods for satiety. Trends
461 Food Sci. Technol. 41, 149–160.
462 Draget, K.I., Skjåk-Bræk, G., Stokke, B.T., 2006. Similarities and differences between
463 alginic acid gels and ionically crosslinked alginate gels. Food Hydrocoll., 7th
464 International Hydrocolloids Conference 20, 170–175.
465 Draget, K.I., Steinsvåg, K., Onsøyen, E., Smidsrød, O., 1998. Na- and K-alginate; effect on
466 Ca2+-gelation. Carbohydr. Polym. 35, 1–6.
467 Dressman, J.B., Berardi, R.R., Dermentzoglou, L.C., Russell, T.L., Schmaltz, S.P., Barnett,
468 J.L., Jarvenpaa, K.M., 1990. Upper gastrointestinal (GI) pH in young, healthy men
469 and women. Pharm. Res. 7, 756–761.
470 Fang, Y., Al-Assaf, S., Phillips, G.O., Nishinari, K., Funami, T., Williams, P.A., 2008.
471 Binding behavior of calcium to polyuronates: Comparison of pectin with alginate.
472 Carbohydr. Polym. 72, 334–341. Fiszman, S., Varela, P., 2013a. The role of gums in
473 satiety/satiation. A review. Food Hydrocoll. 32, 147–154.

474 Fiszman, S., Varela, P., 2013b. The satiating mechanisms of major food constituents – An aid
475 to rational food design. Trends Food Sci. Technol. 32, 43–50.
476 Fraeye, I., Doungla, E., Duvetter, T., Moldenaers, P., Van Loey, A., Hendrickx, M., 2009.
477 Influence of intrinsic and extrinsic factors on rheology of pectin–calcium gels. Food
478 Hydrocoll. 23, 2069–2077.
479 Garrec, D.A., Guthrie, B., Norton, I.T., 2013. Kappa carrageenan fluid gel material
480 properties. Part 1: Rheology. Food Hydrocoll. 33, 151–159.
481 Hermansson, A.-M., Eriksson, E., Jordansson, E., 1991. Effects of potassium, sodium and
482 calcium on the microstructure and rheological behaviour of kappa-carrageenan gels.
483 Carbohydr. Polym. 16, 297–320.
484 Jonassen, H., Treves, A., Kjøniksen, A.-L., Smistad, G., Hiorth, M., 2013. Preparation of
485 Ionically Cross-Linked Pectin Nanoparticles in the Presence of Chlorides of Divalent
486 and Monovalent Cations. Biomacromolecules 14, 3523–3531. Kara, S., Tamerler, C.,
487 Bermek, H., Pekcan, Ö., 2003. Hysteresis During Sol-Gel and Gel-Sol Phase
488 Transitions of k-Carrageenan: A Photon Transmission Study. J. Bioact. Compat.
489 Polym. 18, 33–44.
490 Kopelman, P., 2007. Health risks associated with overweight and obesity. Obes. Rev. 8, 13–
491 17.
492 Kristensen, M., Jensen, M.G., 2011. Dietary fibres in the regulation of appetite and food
493 intake. Importance of viscosity. Appetite 56, 65–70.
494 Lake, A., Townshend, T., 2006. Obesogenic environments: exploring the built and food
495 environments. J. R. Soc. Promot. Health 126, 262–267.
496 Llewellyn, C.H., Wardle, J., 2013. 16 - Satiation and satiety in obesity A2 - Blundell, John
497 E., in: Bellisle, F. (Ed.), Satiation, Satiety and the Control of Food Intake, Woodhead

498 Publishing Series in Food Science, Technology and Nutrition. Woodhead Publishing,
499 pp. 298–315.
500 Logan, K., Wright, A.J., Goff, H.D., 2015. Correlating the structure and in vitro digestion
501 viscosities of different pectin fibers to in vivo human satiety. Food Funct. 6, 62–70.
502 MacArtain, P., Jacquier, J.C., Dawson, K.A., 2003. Physical characteristics of calcium
503 induced κ- carrageenan networks. Carbohydr. Polym. 53, 395–400.
504 Ma, J., Lin, Y., Chen, X., Zhao, B., Zhang, J., 2014. Flow behavior, thixotropy and
505 dynamical viscoelasticity of sodium alginate aqueous solutions. Food Hydrocoll. 38,
506 119–128.
507 Minekus, M., Alminger, M., Alvito, P., Ballance, S., Bohn, T., Bourlieu, C., Carrière, F.,
508 Boutrou, R., Corredig, M., Dupont, D., Dufour, C., Egger, L., Golding, M., Karakaya,
509 S., Kirkhus, B., Feunteun, S.L., Lesmes, U., Macierzanka, A., Mackie, A., Marze, S.,
510 McClements, D.J., Ménard, O., Recio, I., Santos, C.N., Singh, R.P., Vegarud, G.E.,
511 Wickham, M.S.J., Weitschies, W., Brodkorb, A., 2014. A standardised static in vitro
512 digestion method suitable for food – an international consensus. Food Funct. 5, 1113–
513 1124.
514 Morell, P., Fiszman, S.M., Varela, P., Hernando, I., 2014. Hydrocolloids for enhancing
515 satiety: Relating oral digestion to rheology, structure and sensory perception. Food
516 Hydrocoll. 41, 343–353.
517 Muhidinov, Z.K., Fishman, M.L., Avloev, K.K., Norova, M.T., Nasriddinov, A.S., Khalikov,
518 D.K., 2011. Effect of temperature on the intrinsic viscosity and conformation of
519 different pectins. Polym. Sci. Ser. A 52, 1257–1263.
520 Norton, I.T., Frith, W.J., Ablett, S., 2006. Fluid gels, mixed fluid gels and satiety. Food
521 Hydrocoll., 7th International Hydrocolloids Conference 20, 229–239.

522 Norton, J.E., Espinosa, Y.G., Watson, R.L., Spyropoulos, F., Norton, I.T., 2015. Functional
523 food microstructures for macronutrient release and delivery. Food Funct. 6, 663–678.
524 Picout, D.R., Ross-Murphy, S.B., 2003. Rheology of Biopolymer Solutions and Gels. Sci.
525 World J. 3, 105–121. Qin, Y., 2004. Gel swelling properties of alginate fibers. J.
526 Appl. Polym. Sci. 91, 1641–1645.
527 Soukoulis, C., Fisk, I.D., Bohn, T., Hoffmann, L., 2016. Study of intragastric structuring
528 ability of sodium alginate based o/w emulsions under in vitro physiological pre-
529 absorptive digestion conditions. Carbohydr. Polym. 140, 26–34.
530 Spyropoulos, F., Norton, A.B., Norton, I.T., 2011. Self-structuring foods based on acid-
531 sensitive mixed biopolymer to impact on satiety. Procedia Food Sci., 11th
532 International Congress on Engineering and Food (ICEF11) 1, 1487–1493.
533 Ström, A., Schuster, E., Goh, S.M., 2014. Rheological characterization of acid pectin samples
534 in the absence and presence of monovalent ions. Carbohydr. Polym. 113, 336–343.
535 Tecante, A., Nez Santiago, M. del C., 2012. Solution Properties of κ-Carrageenan and Its
536 Interaction with Other Polysaccharides in Aqueous Media, in: De Vicente, J. (Ed.),
537 Rheology. InTech.
538 Thakur, B.R., Singh, R.K., Handa, A.K., Rao, D.M.A., 1997. Chemistry and uses of pectin —
539 A review. Crit. Rev. Food Sci. Nutr. 37, 47–73.
540 Vardakou, M., Mercuri, A., Barker, S.A., Craig, D.Q.M., Faulks, R.M., Wickham, M.S.J.,
541 2011. Achieving Antral Grinding Forces in Biorelevant In Vitro Models: Comparing
542 the USP Dissolution Apparatus II and the Dynamic Gastric Model with Human In
543 Vivo Data. AAPS PharmSciTech 12, 620–626.
544 Vigneri, P., Frasca, F., Sciacca, L., Frittitta, L., Vigneri, R., 2006. Obesity and cancer. Nutr.
545 Metab. Cardiovasc. Dis. 16, 1–7.

546 Wolf, B., Scirocco, R., Frith, W.J., Norton, I.T., 2000. Shear-induced anisotropic
547 microstructure in phase-separated biopolymer mixtures. Food Hydrocoll. 14, 217–
548 225.
549 Yoo, S.-H., Fishman, M.L., Savary, B.J., Hotchkiss, A.T., 2003. Monovalent Salt-Induced
550 Gelation of Enzymatically Deesterified Pectin. J. Agric. Food Chem. 51, 7410–7417.
551 Zhang, S., Zhang, Z., Vardhanabhuti, B., 2014. Effect of charge density of polysaccharides
552 on self-assembled intragastric gelation of whey protein/polysaccharide under
553 simulated gastric conditions. Food Funct. 5, 1829–1838.
554

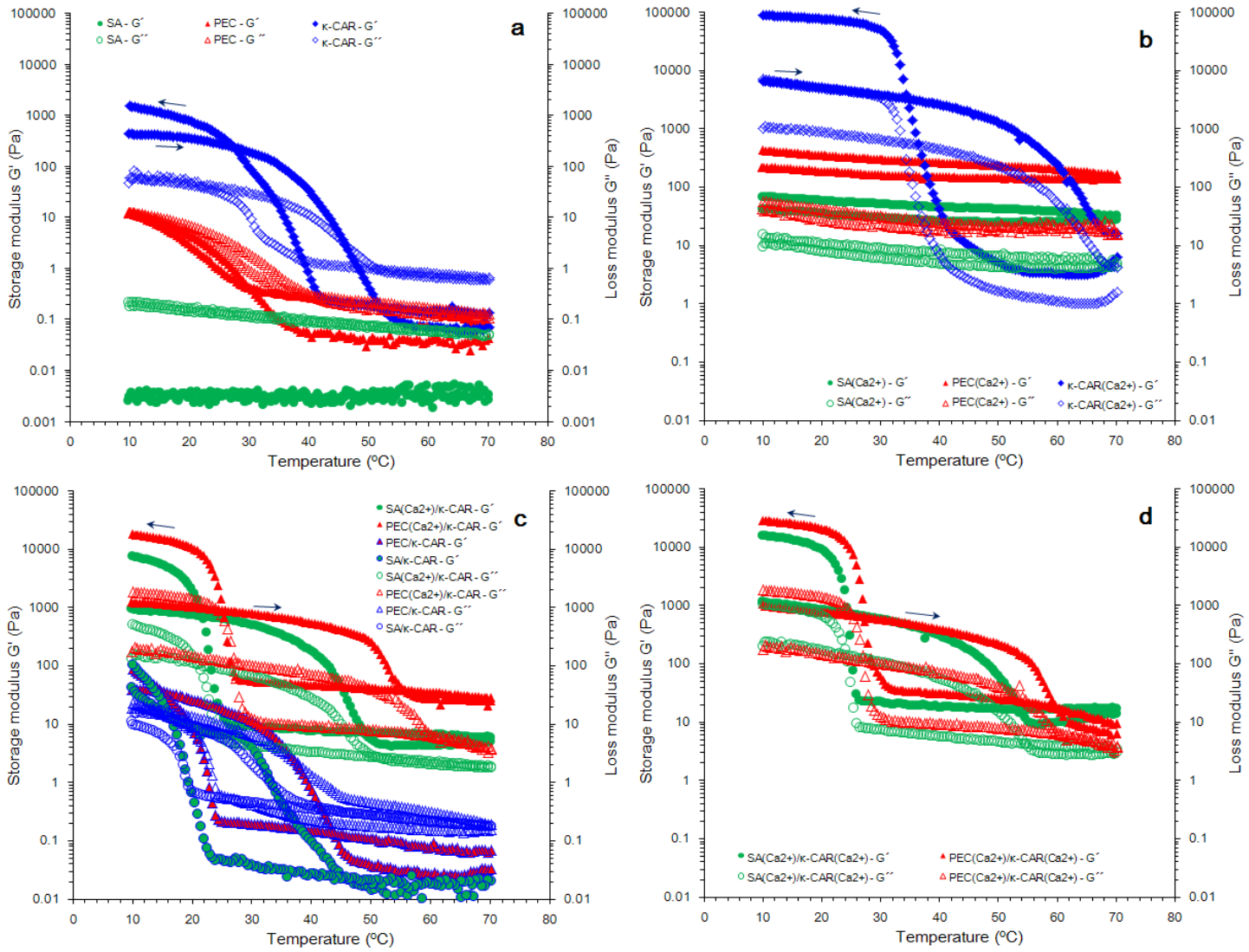
a
SA - G´
SA - G´´
PEC - G´
PEC - G ´´
κ-CAR - G´
κ-CAR - G´´
b
SA(Ca2+) - G´
SA(Ca2+) - G´´
PEC(Ca2+) - G´
PEC(Ca2+) - G´´
κ-CAR(Ca2+) - G´
κ-CAR(Ca2+) - G´´
c
SA(Ca2+)/κ-CAR - G´
PEC(Ca2+)/κ-CAR - G´
PEC/κ-CAR - G´
SA/κ-CAR - G´
SA(Ca2+)/κ-CAR - G´´
PEC(Ca2+)/κ-CAR - G´´
PEC/κ-CAR - G´´
SA/κ-CAR - G´´
d
SA(Ca2+)/κ-CAR(Ca2+) - G´
SA(Ca2+)/κ-CAR(Ca2+) - G´´
PEC(Ca2+)/κ-CAR(Ca2+) - G´
PEC(Ca2+)/κ-CAR(Ca2+) - G´´
Storage modulus G' (Pa)
Loss modulus G'' (Pa)
Temperature (ºC)

FIGURE 1

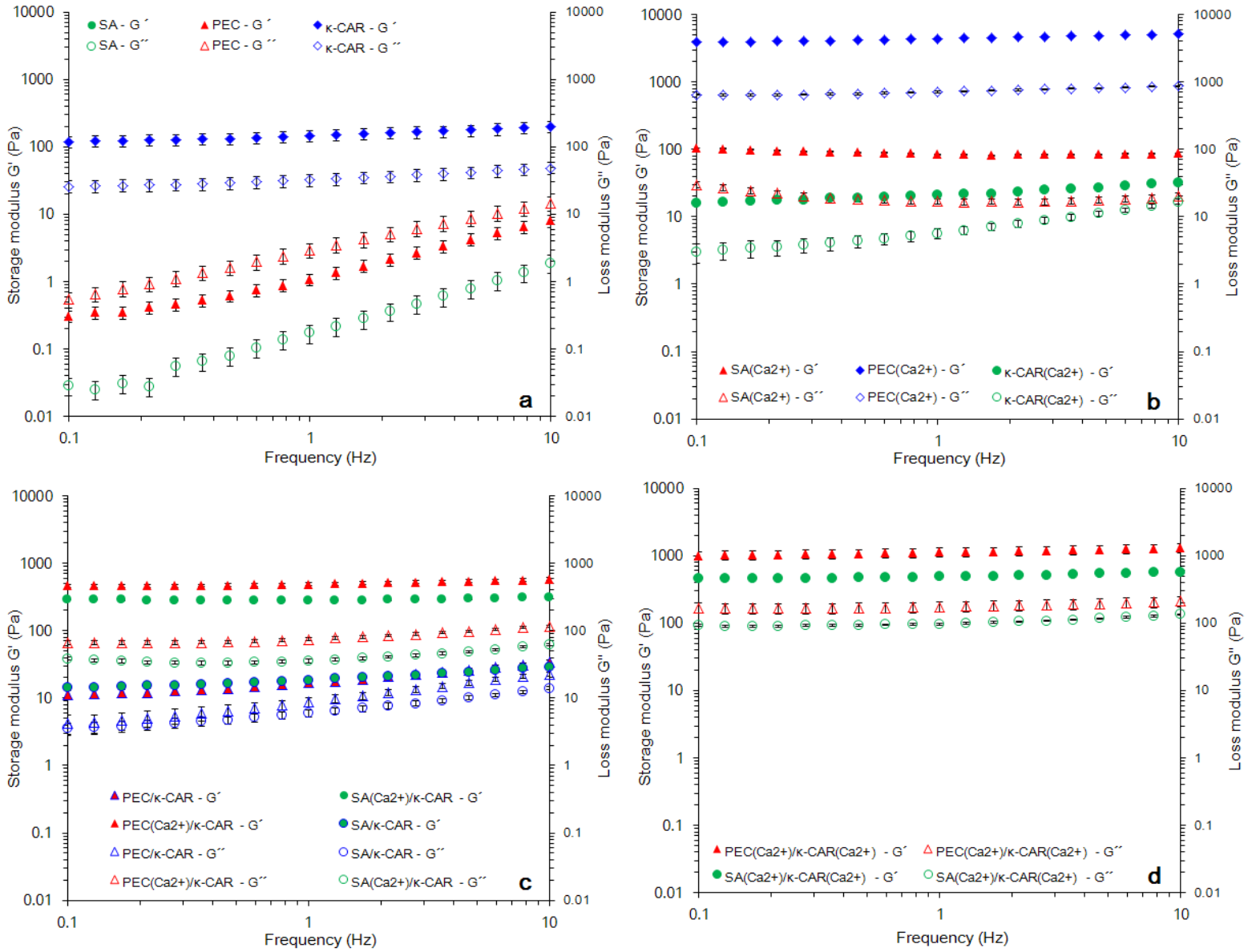
SA - G´
SA - G´´
PEC - G´
PEC - G´´
κ-CAR - G´
κ-CAR - G´´
Storage modulus G' (Pa)
Loss modulus G'' (Pa)
Frequency (Hz)
a
SA(Ca2+) - G´
SA(Ca2+) - G´´
PEC(Ca2+) - G´
PEC(Ca2+) - G´´
κ-CAR(Ca2+) - G´
κ-CAR(Ca2+) - G´´
b
PEC/κ-CAR - G´
PEC(Ca2+)/κ-CAR - G´
PEC/κ-CAR - G´´
PEC(Ca2+)/κ-CAR - G´´
SA(Ca2+)/κ-CAR - G´
SA/κ-CAR - G´
SA/κ-CAR - G´´
SA(Ca2+)/κ-CAR - G´´
c
PEC(Ca2+)/κ-CAR(Ca2+) - G´
PEC(Ca2+)/κ-CAR(Ca2+) - G´´
SA(Ca2+)/κ-CAR(Ca2+) - G´
SA(Ca2+)/κ-CAR(Ca2+) - G´´
d

FIGURE 2

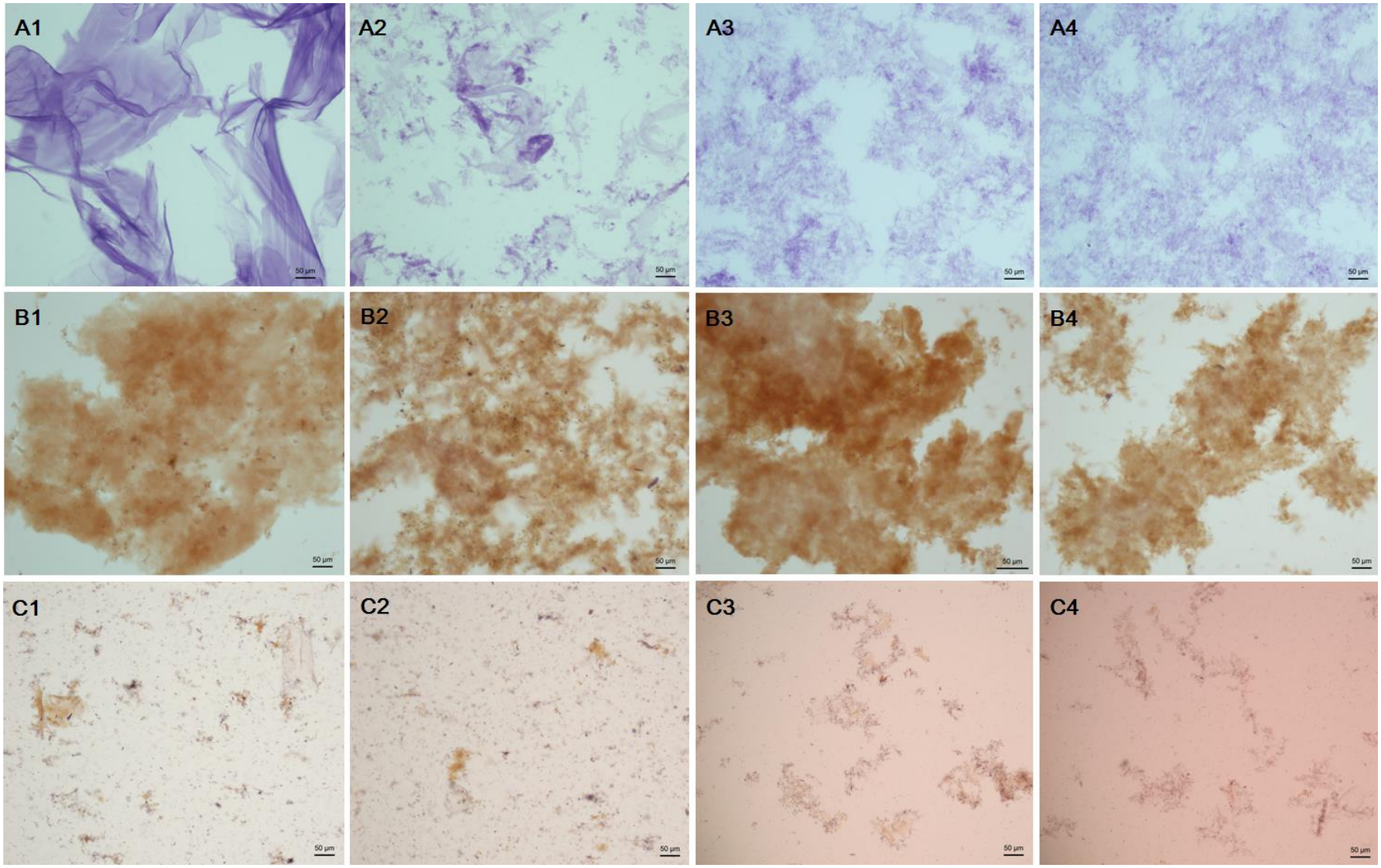

FIGURE 3

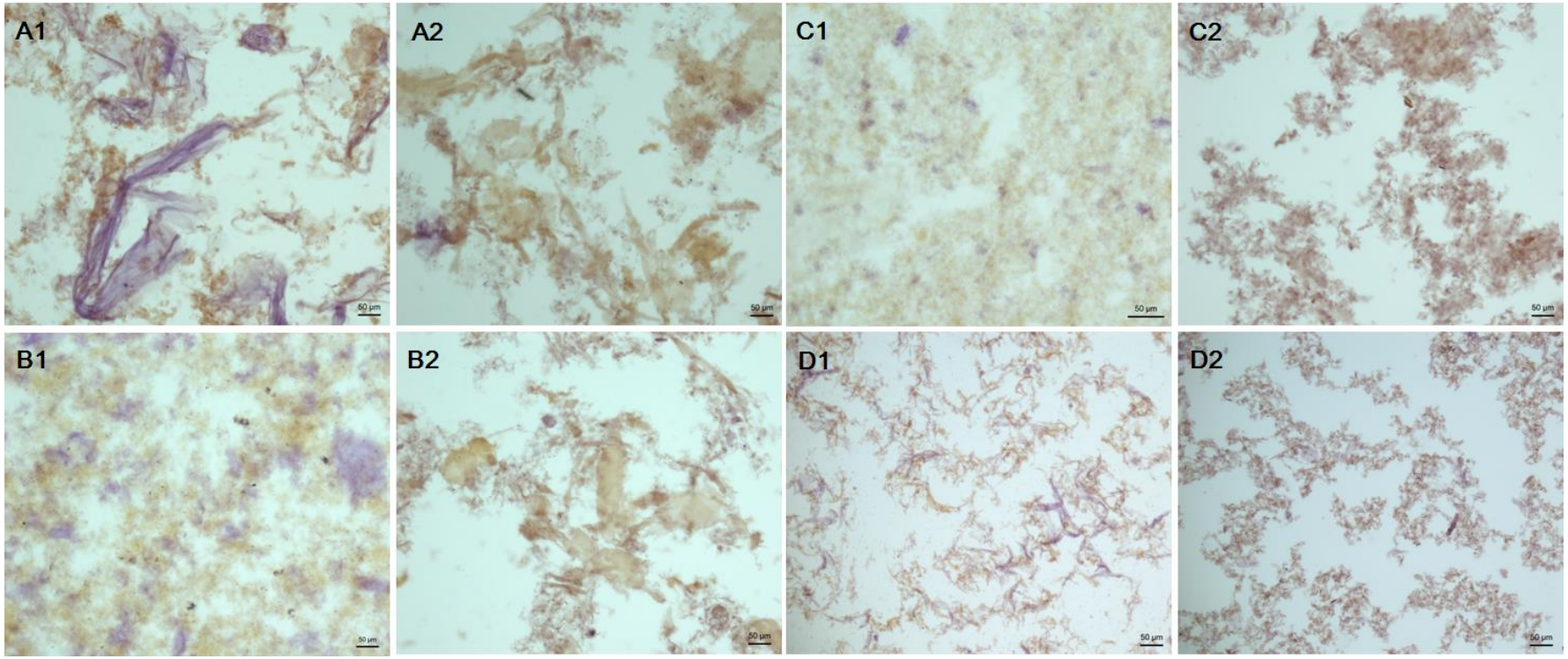

FIGURE 4

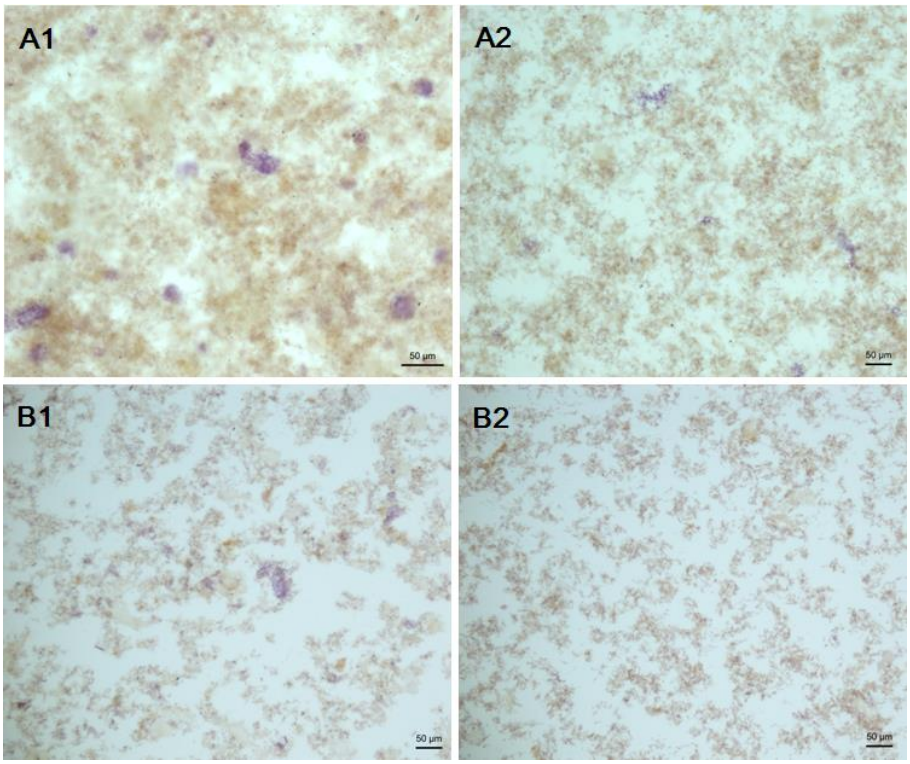

FIGURE 5

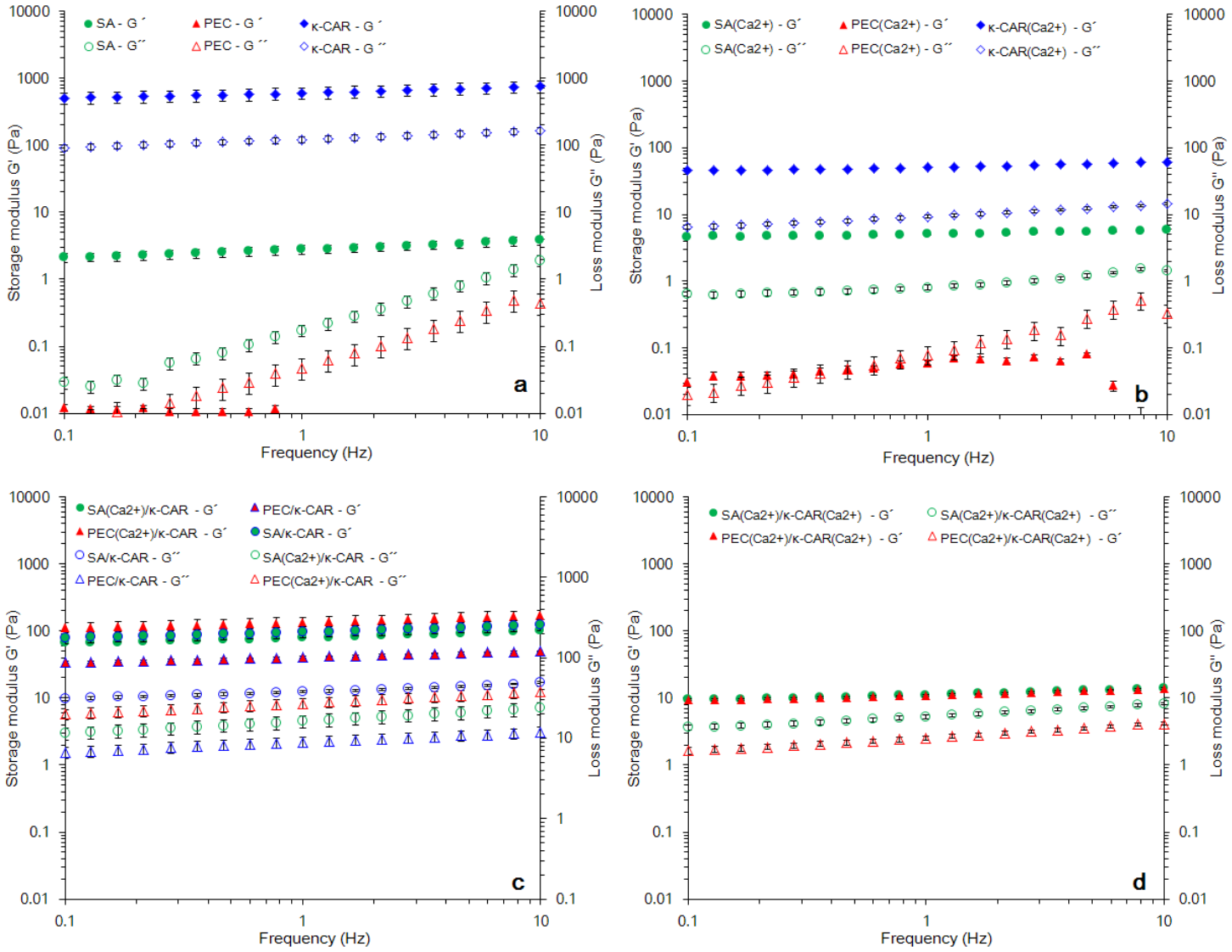
SA - G´
PEC - G´
κ-CAR - G´
SA - G´´
PEC - G´´
κ-CAR - G´´
Storage modulus G' (Pa)
Loss modulus G'' (Pa)
Frequency (Hz)
a
SA(Ca2+) - G´
PEC(Ca2+) - G´
κ-CAR(Ca2+) - G´
SA(Ca2+) - G´´
PEC(Ca2+) - G´´
κ-CAR(Ca2+) - G´´
b
SA(Ca2+)/κ-CAR - G´
PEC/κ-CAR - G´
PEC(Ca2+)/κ-CAR - G´
SA/κ-CAR - G´
SA/κ-CAR - G´´
SA(Ca2+)/κ-CAR - G´´
PEC/κ-CAR - G´´
PEC(Ca2+)/κ-CAR - G´´
c
SA(Ca2+)/κ-CAR(Ca2+) - G´
SA(Ca2+)/κ-CAR(Ca2+) - G´´
PEC(Ca2+)/κ-CAR(Ca2+) - G´
PEC(Ca2+)/κ-CAR(Ca2+) - G´
d

FIGURE 6

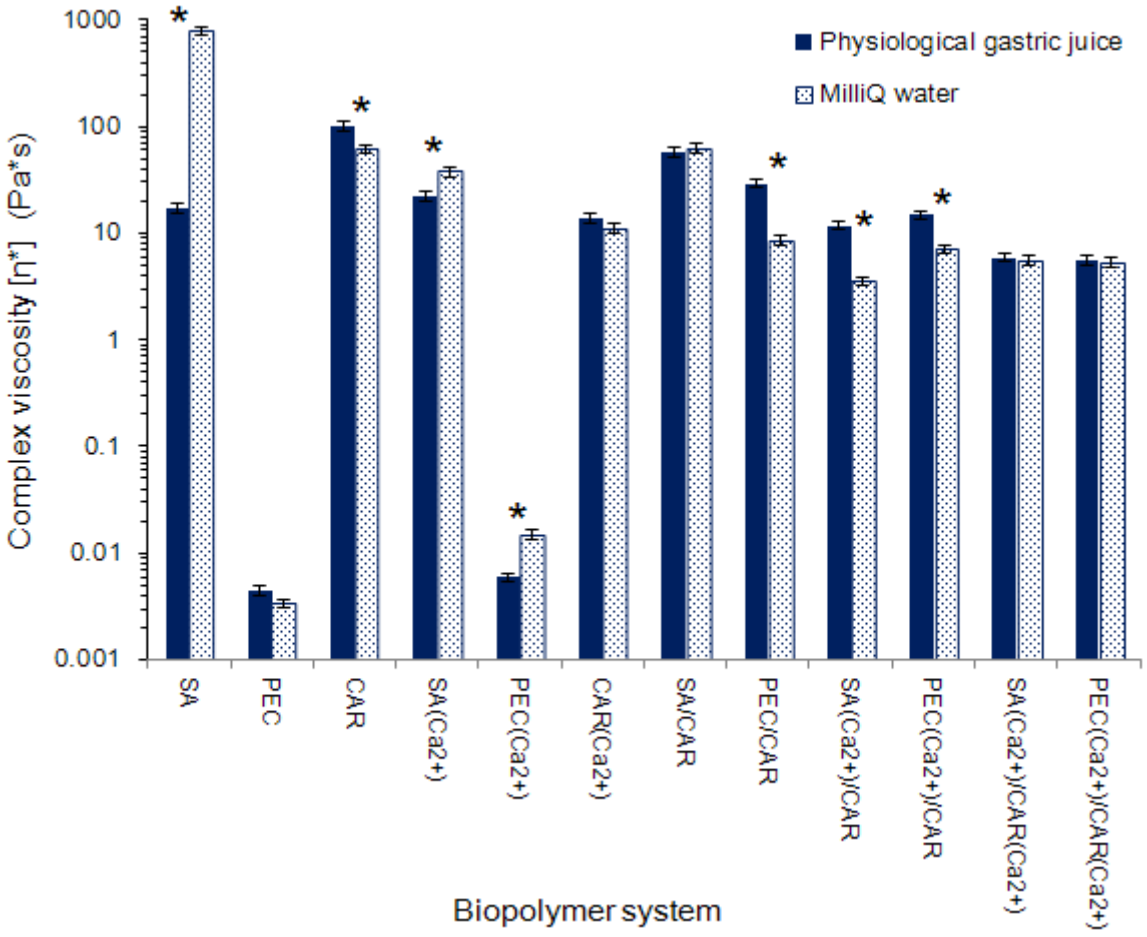
Physiological gastric juice
MilliQ water
Complex viscosity [η*] (Pa*s)
1000
100
10
1
0.1
0.01
0.001
*
SA
PEC
CAR
SA(Ca2+)
PEC(Ca2+)
CAR(Ca2+)
SA/CAR
PEC/CAR
SA(Ca2+)/CAR
PEC(Ca2+)/CAR
SA(Ca2+)/CAR(Ca2+)
PEC(Ca2+)/CAR(Ca2+)
Biopolymer system

FIGURE 7

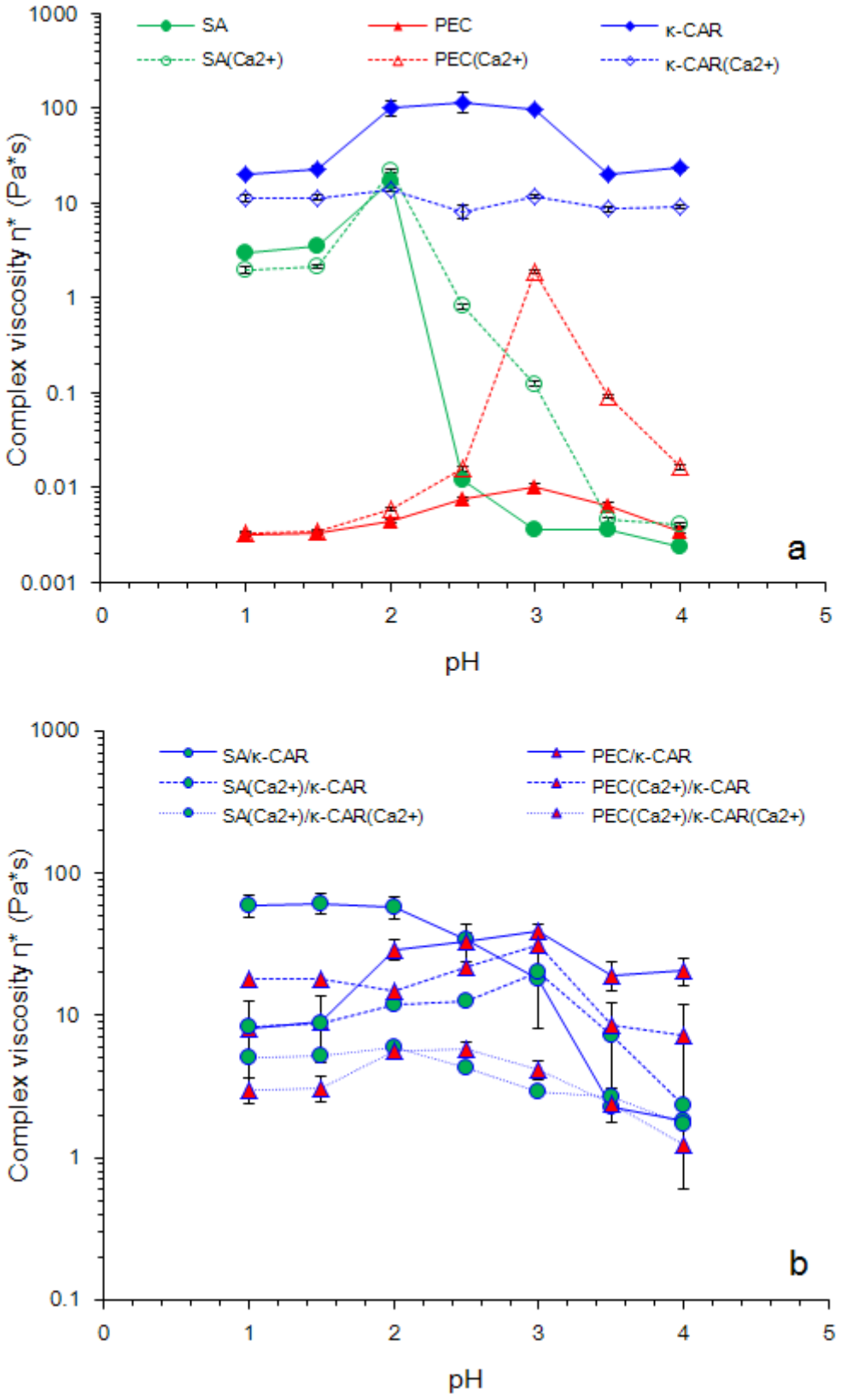
SA
PEC
κ-CAR
SA(Ca2+)
PEC(Ca2+)
κ-CAR(Ca2+)
Complex viscosity η* (Pa*s)
1000
100
10
1
0.1
0.01
0.001
0
1
2
3
4
5
pH
a
SA/κ-CAR
PEC/κ-CAR
SA(Ca2+)/κ-CAR
PEC(Ca2+)/κ-CAR
SA(Ca2+)/κ-CAR(Ca2+)
PEC(Ca2+)/κ-CAR(Ca2+)
Complex viscosity η* (Pa*s)
1000
100
10
1
0.1
0
1
2
3
4
5
pH
b

FIGURE 8

SUPPLEMENTARY TABLE 1

Sample	Gelation gel temperature T_{gel} (˚C)	Melting point temperature T_{gel} (˚C)
SA	nd†	nd
PEC	nd	nd
κ-CAR	38.9 ± 0.5^{b}	46.2 ± 0.7^{c}
SA/κ-CAR	21.0 ± 0.4^{a}	19.5 ± 0.2^{a}
PEC/ κ-CAR	20.5 ± 0.9^{a}	36.0 ± 0.4^{b}
SA-Ca^{2+}	nd	nd
PEC-Ca^{2+}	nd	nd
κ-CAR-Ca^{2+}	nd	nd
SA-Ca^{2+}/CAR	nd	nd
PEC-Ca^{2+}/CAR	nd	nd
SA-Ca^{2+}/CAR-Ca^{2+}	nd	nd
PEC-Ca^{2+}/CAR-Ca^{2+}	nd	nd